ISSN 0001-4370, Oceanology, 2006, Vol. 46, No. 3, pp. 299–304. © Pleiades Publishing, Inc., 2006.
Original Russian Text © I.D. Lozovatsky, S.M. Shapovalov, 2006, published in Okeanologiya, 2006, Vol. 46, No. 3, pp. 325–330.

MARINE PHYSICS

Parameterization of the Depth of the Upper Quasi-Homogeneous Layer Based on Measurements in the North Atlantic (Section Along 53° N)

I. D. Lozovatsky and S. M. Shapovalov

Shirshov Institute of Oceanology, Russian Academy of Sciences, Moscow, Russia
e-mail: smsphap@ocean.ru

Received December 22, 2004; in final form, June 15, 2005

Abstract—The dependence of the variation in the depth of the upper mixed layer (MLD) on the governing parameters (the momentum flux, the buoyancy fluxes at the ocean surface, and the density gradient in the pycnocline) is considered. It is shown that, in the spring storm season, wind mixing dominates over convective mixing. In this case, the MLD is linearly correlated with the Ekman scale calculated from the friction velocity observed approximately 12 h before the measurement of the MLD.

DOI: 10.1134/S0001437006030015

1. INTRODUCTION

The seasonal variations in the atmospheric forcing of the ocean are most clearly manifested at the mid-latitudes of the Northern Hemisphere between 40° and 60° N. During the warm season (late spring–early autumn), the heat flux is directed from the atmosphere to the ocean, whereas, in the winter and early spring, the major part of the North Atlantic Current is subjected to a stable influence of a negative (upward) heat flux. The convective exchange between the ocean and the atmosphere, combined with the prevailing strong winds, generates and maintains turbulence in the upper quasi-homogeneous layer (UHL). In April 2001, measurements of the vertical structure in the UHL over a zonal transoceanic section at the boundary between the high and mid-latitudes were carried out during cruise 9 of R/V *Akademik Ioffe* using a Neil Brown Mark III CTP profiler. The CTD profiles were obtained at 42 stations located approximately along 53° N from the coast of Labrador to the shelf of Ireland. The mean distance between the stations was 30 miles, and the mean time interval between the profiles was 6 h [4]. The sensors of the CTD profiler were calibrated at a laboratory setup of the Federal Department of Marine Navigation and Hydrography (Bundesamt fur Seeschiffahrt und Hydrographie (BSH)) in Hamburg. The data obtained were processed according to the standards of the WOCE program. The meteorological parameters were permanently recorded by a Wetos 625 automatic meteorological station on the ship.

In this study, the main attention is focused on the analysis of the variability of the UHL depth under the influence of the prevailing storm winds and convective buoyancy flux in the winter–spring period.

2. METEOROLOGICAL CONDITIONS

The meteorological conditions along the section were determined by relatively strong winds and a negative heat balance at the ocean surface (a positive heat balance was observed only at two stations). The buoyancy flux J_b and wind stress $|\tau_a| = (\tau_x^2 + \tau_y^2)^{1/2}$ at each drift station are shown in Fig. 1. The positive values of $-J_b$ correspond to the conditions favorable for the development of convection. The calculations of the J_b and $|\tau_a|$ were performed using the Mathlab Air-Sea Toolbox (http://sea-mat.whoi.edu) software, which realizes bulk-formulas for the fluxes at the water–air boundary. We note that Fig. 1 is based on the meteorological data obtained only at drift stations when the wind speed did not exceed 17 m/s. The average wind speed at the stations was W_{ast} = 8.7 m/s at the root-mean-square values rmsW_{ast} = 4.6 m/s. Combining the data of the measurements at the stations with the data obtained during the tacks between the stations yields a mean wind speed of $\langle W_a \rangle$ = 10.7 m/s. On April 19–20 (between stations 923 and 926) and on April 27–28 (between stations 952 and 954), two periods of severe storm weather were recorded with the wind speeds exceeding 12 m/s. On April 28, 2001, the maximal wind velocity $W_{\max}$ = 29 m/s was recorded. Two shorter storms were observed between stations 933 and 935 (at night on April 22, $W_{\max}$ = 26 m/s) and stations 941–942 (on April 24, $W_{\max}$ = 13 m/s). The peak values of $|\tau_a|$ and the wind energy at an altitude of 10 m over the sea level $E_{10} = W_a \tau_a^2$ reached 0.2–0.4 N/m^2 and 4–6 W/m^2, respectively.

The temperature of the sea surface exceeded the air temperature at each station, which, being combined with strong winds, provided for the domination of a

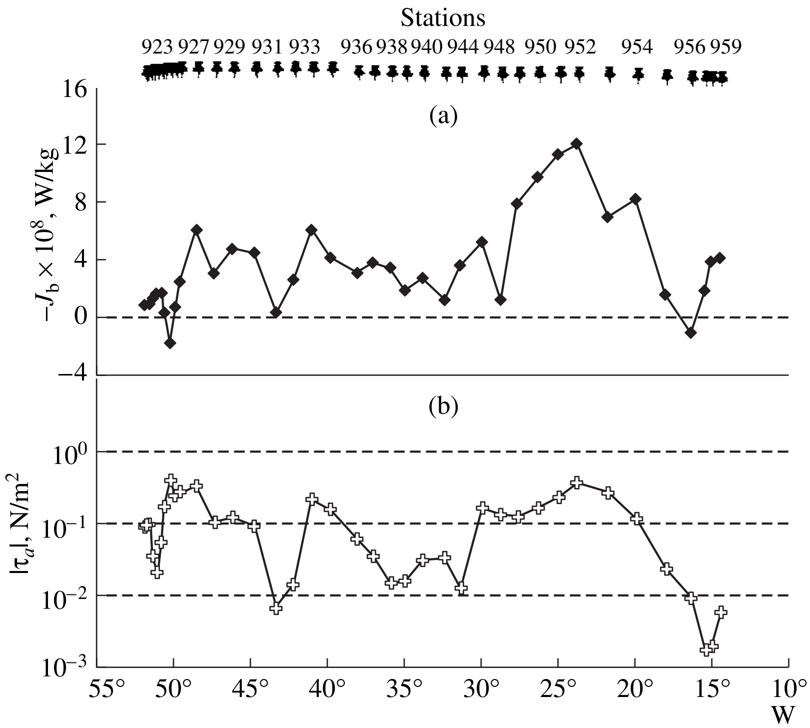

Fig. 1. Meteorological data: (a) buoyancy flux J_b and (b) wind stress $|\tau_a|$ at drift stations along the section (the positive values of $-J_b$ correspond to the negative heat balance at the ocean surface).

negative heat balance along the section. The mean difference was $\Delta T_{wa} = T_w - T_a = 2.55°C$, while rms$\Delta T_{wa}$ = 1.57°C.

3. DETERMINATION OF THE MIXED LAYER DEPTH

The modern stage of researching the depth of the upper quasi-homogeneous (mixed) layer of the ocean coincides with the beginning of the application of high-resolution thermohaline profilers for profiling the thermohaline water structure (the end of the 1960s–the beginning of the 1970s). A summarizing analysis of the UHL depth in the northern part of the Pacific Ocean based on the standard hydrographic data performed by that time was presented in [5]. A description of the main methods for identification of the UHL lower boundary can be found in [1, 2]. Attempts to contrive universal methods for distinguishing the UHL for automated processing of large arrays of hydrographic data have been continuing in the last decade (see, for example, [6, 10]). We note that the majority of the methods suggested were aimed at the analysis of standard hydrographic stations with relatively low vertical resolution (not better than 10 m in the upper layer). Approximation of the profiles in the transition zone from the UHL to the thermocline by one or another polynomial functions [6] makes it possible to obtain estimates of the UHL depth that satisfy the requirements of the analysis of its seasonal and regional variability. Fast synoptic variations in the UHL require, in our opinion, application of more local criteria. Below, we shall briefly summarize the main approaches to the calculation of the UHL depth that were used to choose the method [10] best corresponding to the character of the data analyzed here.

The depth of the UHL z_D can be determined as the depth at which the absolute value of the difference between $T(z_D)$ and the surface temperature T_w does not exceed a preset fixed value δT. According to this definition, the UHL depth is the isothermal layer depth (ILT) [10]. When this approach is applied to the density profiles, z_D is interpreted as the mixed layer depth (MLD), where the absolute value of the density difference $\delta\sigma_\theta = |\sigma_\theta(z_D) - \sigma_{\theta w}|$ is smaller than a preset value of $\delta\sigma_\theta$. The authors of [19, 32] calculated the UHL depth with relatively small values (δT = 0.2 and 0.1°C, respectively). The threshold difference δT = 0.5°C was used in [11, 21, 23, 27], while the authors of [12, 28, 33] used δT = 1°C. The most typical value of the density difference $\delta\sigma_\theta$ for the calculation of the MLD is within $(0.10–0.13)\sigma_\theta$ [9, 14, 15, 20, 31], whereas the authors of [24, 25, 30] use a more strict restriction $\delta\sigma_\theta = (0.01–0.03)\sigma_\theta$.

The MLD can also be defined as the depth of the layer in which the vertical gradient of the temperature or of the conventional density is smaller than the characteristic preset values $\delta T/\delta z$ or $\delta\sigma_\theta/\delta z$. It is assumed that a thin interface exists between the UHL and the underlying thermohalocline [5–8, 18, 29]. The threshold gradients are usually set in the range 0.02–0.05°C/m for $\delta T/\delta z$ and 0.01 kg/m^4 for $\delta\sigma_\theta/\delta z$. The algorithm for calculating the MLD suggested in [10] combines the application of the criteria δT and $\delta\sigma_\theta$ with an additional condition that the values of the temperatures (or densities) at adjacent sequential levels differ by less than $0.1\delta T$ and $0.1\delta\sigma_\theta$. This approach can be called local, which makes it possible to sufficiently accurately determine the MLD on the basis of high-resolution profile measurements.

It is noteworthy that the application of one or another formal criterion for calculating the MLD can lead to notable errors if the dataset analyzed is significantly nonuniform (see the discussion in [8]). Combining the profiles with the sharp and weak pycnoclines that underlie the mixed layer creates a problem of using unified δT or $\delta\sigma_\theta$ values for identification of the MLD. Thus, if a limited data set is analyzed, it is useful to verify the results of formalized calculations of the MLD visually or, if necessary, to correct them manually. In our work with the temperature and density profiles, we followed such an approach using the criteria δT and $\delta\sigma_\theta$ at the initial stage and then visually estimating each individual profile. Calculations of the MLD (from hereon the h_D) were performed with the initial value $\delta\sigma_\theta = 0.02\sigma_\theta$ and manual correction of the MLD was required only for four profiles. Calculations of the isothermal layer depth were performed using the algorithm given in [10] with ΔT varying within 0.1–0.3°C with a step of 0.05°C. The best agreement between h_D and ILT without any vertical averaging and interpolation was reached at $\Delta T = 0.25$°C. In this case, the linear correlation between the MLD and ILT is characterized by a high statistical reliability ($r^2 = 0.95$). In the further analysis, we use the estimates of the MLD obtained using the differential approach with a manual correction for a more precise identification of the transition zone between the mixed layer and the thermohalocline. These estimates of the mixed layer depth vary from 6 to 110 m.

4. VARIATIONS IN THE MIXED LAYER DEPTH

Variations in the MLD (h_D) along the section are shown in Fig. 2. The mean $\tilde{h}_D = 44.5$ m, the median med(h_D) = 48 m, and the rms(h_D) = 25.2 m. The maximal $h_D = 110$ m was observed at station 931. Three intervals can be distinguished in Fig. 2 (between stations 924–931, 936–938, and 949–956) with a notable increase in the depth of the mixed layer ($h_D > 50$ m). Three periods of wind increase ($W_a > 10$ m/s) correspond to these intervals, which, however, precede in time (space) the periods of deepening of the lower boundary of the mixed layer (Fig. 2). Since the value of $-J_b$ also increases with the increasing wind speed (Fig. 1) (i.e., the probability of the development of convective mixing increases), we tried to determine the ratio of the contribution of the atmospheric momentum flux (the friction velocity u_*) and the buoyancy to the variation of the MLD by calculating the cross correlation functions $R_{hu_*}(\Delta t)$ and $R_{hJ_b}(\Delta t)$, where Δt is the corresponding time shift. In order to perform these calculations, it was necessary to form series of MLD and flux values with uniform spatial spacing. Since the measurements were carried out at 42 points in 12 days, we took a time step for the interpolation equal to Δt_{int} = 6 h, which provided approximately the same number of interpolation points (49). Regarding the data for correlation analysis as time series rather than as spatial variables, we proceed from the assumption that the main cause for the variation in the depth of the mixed layer at 53° N is related to the synoptic scale of the variability of u_* and J_b caused by the storms. The length of the regions in which the MLD exceeds 50 m is equal to 250–350 km, which agrees with the width of the fronts of the atmospheric cyclones at these latitudes.

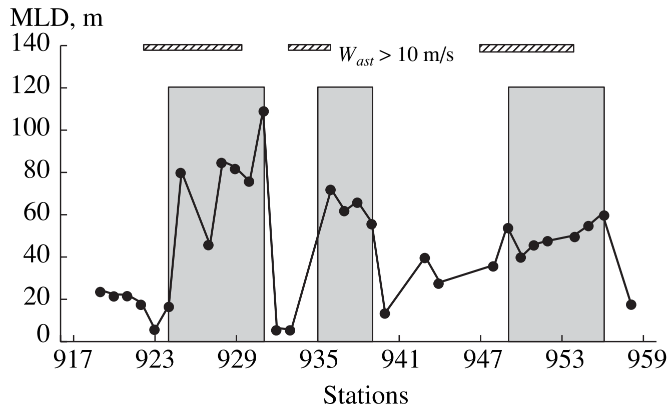

Fig. 2. Variations of the MLD along the section. The periods of the MLD deepening (the dashed intervals) occur with a time lag with respect to the periods of the wind enhancement (W_{ast} > 10 m/s), which is shown along the upper axis.

The correlation between h_D and $-J_b$ appeared below the 95% confidence level ($R_{0.95} = 0.34$) for all the Δt except for $\Delta t = 0$, at which max $R_{hJ_b}(0) = 0.4$ only slightly exceeded $R_{0.95}$. Meanwhile, a statistically reliable correlation maximum $R_{hu_*}(\Delta t) = 0.71$ was found between the variations of h_D and the friction velocity u_* at the time shift $\Delta t = 12$ h. We note that, according to the data in [13], the maximal correlation between the wind stress and the MLD in the waters of the coastal upwelling was also observed at a nonzero time shift Δt, which varied in the range from 5–6 to 10–12 h depending on the synoptic situation.

The results of the correlation analysis allow us to suppose that the observed depths of the mixed layer were mainly determined by the wind stress shifted in time (space), whereas the influence of the buoyancy

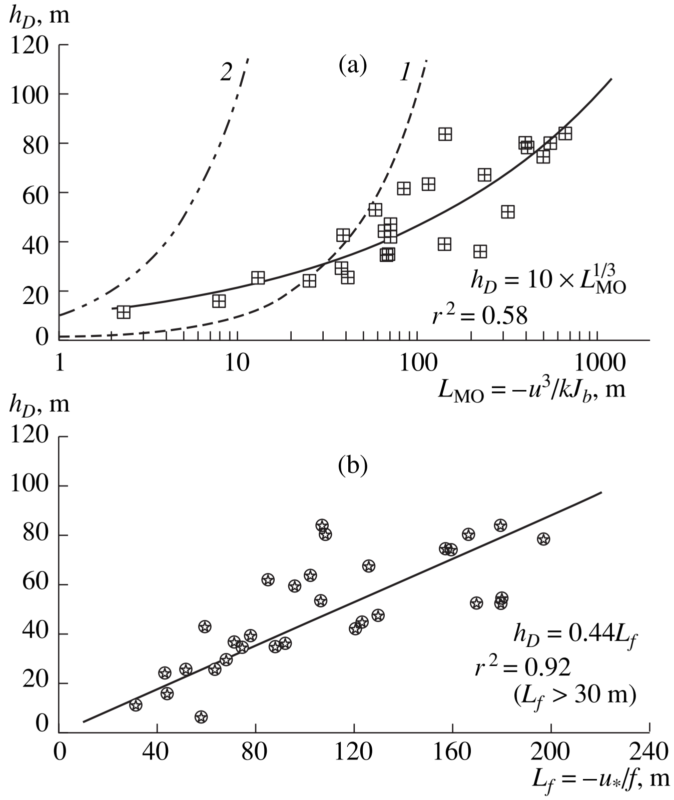

Fig. 3. Correlation of the MLD h_D with the (a) Monin–Oboukhov scales L_{MO} and (b) Ekman scale L_f for estimates of the wind stress u_* taken with a time delay equal to 12 h. In both cases, the times of the measurements of the MLD and the buoyancy flux J_b coincide. The functions $h_D/L_{MO} = 1$ and 10 are shown with (*1*) dashed lines and (*2*) dotted–dashed lines. For synchronous measurements of the h_D and u_*, no correlation is observed between the MLD and the L_{MO} and L_f scales. The scale L_{MO} is calculated only for stations 926–954.

loss in the surface layer was comparatively weak. This conclusion is also confirmed by the analysis of the dependence of h_D on the scale of the Monin–Oboukhov length $L_{MO} = -u_*^3/\kappa J_b$ shown in Fig. 3a. The data of the observations were compared in Fig. 3a with the functions $h_D/L_{MO} = 1$ and $h_D/L_{MO} = 10$, which, according to [16], limit the range of the h_D variability, where the influence of the wind stress on the development of the MLD is comparable with the influence of the convective buoyancy flux. At $h_D/L_{MO} > 1$ (to the left of line *2*), convection should manifest a dominating influence on the MLD, while at $h_D/L_{MO} < 1$ (to the right of line *1*), wind stress is the prevailing factor. Only at three stations (where $h_D < 35$ m), the contributions of the wind stress and buoyancy flux to the formation of the mixed layer depth are comparable. The majority of the points in Fig. 3a are located below the line $h_D/L_{MO} = 1$ pointing to the fact that convection in the spring period in the North Atlantic is a secondary factor as compared to the mixing caused by the wind. Since $L_{MO} \sim u_*^3$, the approximating function $h_D = 10L_{MO}^{1/3}$ shown in Fig. 3a points to a linear correlation between the MLD and the friction velocity. The buoyancy flux in this case actually plays the role of a scaling factor.

The result obtained allows us to use a simpler dependence for the parameterization of the MLD: $h_D(L_f)$, where $L_f = u_*/f$ is the Ekman scale (Fig. 3b), which is well approximated by the linear function $h_D \approx 0.44L_f$ if h_D is shifted back by $\Delta t = 12$ h with respect to the changes in the friction velocity u_*. Simultaneous measurements of u_* and h_D do not demonstrate any significant dependence between h_D and L_{MO} and between h_D and L_f. Figure 3 points to the fact that the wind stress related to the spring storms in the North Atlantic should act during ~12 h to mix the existing stratification and to form a UHL with a mean depth of ~45 m. The physical mechanism of such mixing may be related, in particular, to the vertical gradients of the velocity induced by the inertial oscillations at the lower boundary of the UHL [26]. In our case, a transition time close to $\Delta t \approx 12$ h is needed for reaching the steady state of this process. This is the so-called spin-up interval counted from the moment of the beginning of the wind perturbation (storm). The interpretation suggested assumes a quasi-stationary state of the observed mixed layer, when its depth does not change very fast. At some stations, especially at those that were occupied at the beginning of storms, this condition was obviously not observed. This can explain, in particular, the scattering of the data near the linear trend shown in Fig. 3b.

One-dimensional models of the thermocline deepening [17, 22, 27, and others] that use a constant wind stress and a zero buoyancy flux predict a fast increase in the MLD only in the first half of the inertial period, i.e., in our case, for approximately 7–8 h ($\tau_{in} \approx 15$ h at 53° N). Later, the increase in the UHL depth significantly drops, changing in time as $h_D/L_{fN} \sim (t/\tau_{in})^{1/4}$ [17], where $L_{fN} = u_*/\sqrt{f\tilde{N}_{pc}}$ is the characteristic scale, which can be called the stratified Ekman scale ($\tilde{N}_{pc}$ is the mean buoyancy frequency in the pycnocline). According to [26], this scale parameterizes the influence of the nonlocal (u_*) and local ($\tilde{N}_{pc}$) processes on the variations in h_D. The scale L_{fN} was used in [13, 34], as well as in the study of the boundary atmospheric layers [35]. We note that the correlation between the MLD and the depth of the maximum of the density gradient in the thermocline is the basis of the method for distinguishing the UHL suggested in [6].

According to our data, the ratio $h_D/L_{fN} \approx 1.9$, whereas the authors of [26] obtained an estimate for h_D/L_{fN} equal to 1.7, and the authors of [34] give a value of 1.3. The authors of [17] showed that h_D/L_{fN} tends to 1.7 after the wind stress reaches a steady state. The agreement between the empirical and model estimates of the h_D/L_{fN} ratio confirms the conclusion that, at the majority of stations, the mixed layer was observed in the latest stage of its development close to the equilibrium state.

The high degree of linearity between the MLD and the Ekman scale points to the fact that atmospheric forcing is the main cause of the UHL formation and the variation in its depth along the section. The calculations of the ageostrophic currents performed in [3] (using the data of a shipborne acoustic velocity profiler) showed that the depth of the drift current penetration at the stations of the section generally coincides with the MLD. This fact also confirms the dominating influence of the wind mixing on the formation of the UHL during the period of the observations. Local horizontal and thermohaline gradients in the upper layer could cause distortions in the structure of the UHL; however, obviously, the scales of the UHL variability analyzed (from a few tens of miles to a few tens of hours) were predominantly determined by the variations in the wind stress related to the high storm activity in the North Atlantic during the transition season from the winter to the summer. At the same time, the variations in the wind stress vorticity along 53° N on the basin scale determined the generally observed deepening of the thermocline from the west to the east.

5. CONCLUSION

The variability of the depth of the upper mixed layer was analyzed on the basis of profile measurements of the thermohaline structure at 42 hydrographic stations in the Atlantic Ocean in the spring of 2001 along 53° N. Identification of the MLD was performed using the modified method of the threshold density difference [10] supplemented by expert inspection. The mean value of the MLD appeared to be equal to 45 m; the maximal value was 110 m. The variations in the MLD were compared to the variations in the momentum and buoyancy fluxes at the ocean surface and in the density gradient in the pycnocline.

The maximal correlation (0.71) between the MLD and the friction velocity at the ocean surface u_* was found at a time shift equal to 12 h. The correlation between the MLD and the buoyancy flux appeared to be statistically insignificant. The analysis of the dependence of the MLD on the Monin–Oboukhov scale showed that the formation of the mixed layer in the period of the observations occurred mainly under the influence of the wind rather than the convective mixing. The dependence of the MLD (h_D) on the Ekman scale $L_f = u_*/f$ is expressed by the linear function $h_D \approx 0.44L_f$ with a high regression coefficient, $r^2 = 0.92$. The result obtained indicates that the formation of the upper mixed layer with a depth of approximately 45 m at a mean friction velocity $\langle u_* \rangle = 1.2 \times 10^{-2}$ m/s requires approximately 12 h of wind forcing.

Application of the "stratified" Ekman scale $L_{fN} = u_*/\sqrt{f\tilde{N}_{pc}}$ for parameterization of the MLD leads to the relation $h_D \approx 1.9L_{fN}$. This result agrees with the model calculations of the MLD for the late (slow) stage of the mixed layer evolution under stationary wind forcing indicating that the UHL at the majority of the stations was observed at a state close to the equilibrium one. Therefore, the L_{fN} can be a good indicator of the MLD for the UHL formed by storm wind.

ACKNOWLEDGMENTS

This study was supported by the Russian Foundation for Basic Research (project no. 02-05-64408) and Arizona State University. The authors thank the anonymous reviewer whose remarks helped to improve the presentation of the paper.

REFERENCES

1. V. I. Kalatskii, *Modeling Vertical Thermal Structure of the Active Ocean Layer* (Gidrometeoizdat, Leningrad, 1978) [in Russian].
2. A. A. Kuznetsov, *Upper Quasihomogeneous Layer of the North Atlantic* (IOAN–VNIIGMI–MTsD, Obninsk, 1982) [in Russian].
3. I. D. Lozovatskii, S. M. Shapovalov, and E. Ruzhe, "Ageostrophic Dynamics of the Upper Layer of the Ocean: Measurements over Transatlantic Section along 53° N," Okeanologiya **46** (1), 5–13 (2006) [Oceanology **46**, (1), 5–13 (2006)].
4. V. P. Tereshchenkov, S. M. Shapovalov, S. A. Dobrolyubov, and E. G. Morozov, "Cruise 9 of R/V *Akademik Ioffe*," Okeanologiya **42** (2), 315–318 (2002) [Oceanology **42** (2), 298–301 (2002)].
5. B. N. Filyushkin, "Thermal Characteristics of the Upper Water Layer in the Northern Part of the Pacific Ocean," Okeanologicheskie Issledovaniya (Mezhduved. Geofiz. Komitet AN SSSR), No. 19, 22–69 (1968).
6. B. N. Filyushkin, N. A. Dianskii, and S. N. Moshonkin, "Determination of the Lower Boundary of the Upper Mixed Layer of the Ocean," Okeanologiya **36** (1), 133–137 (1996) [Oceanology **36** (1), 122–126 (1996)].
7. K. H. Bathen, "On the Seasonal Changes in the Depth of the Mixed Layer in the North Pacific Ocean," J. Geophys. Res. **77**, 7138–7150 (1972).
8. K. E. Brainerd and M. C. Gregg, "Surface Mixed and Mixing Layer Depths," Deep-Sea Res. **42** (9), 1521–1544 (1995).
9. R. X. Huang and S. Russell, "Ventilation of the Subtropical North Pacific," J. Phys. Oceanogr. **24** (12), 2589–2605 (1994).
10. A. B. Kara, P. A. Rochford, and H. E. Hurlburt, "An Optimal Definition for Ocean Mixed Layer Depth," J. Geophys. Res. **105**, 16 803–16 821 (2000).
11. K. A. Kelly and B. Qiu, "Heat Flux Estimates for the Western North Atlantic, I, Assimilation of Satellite Data

Into a Mixed Layer Model," J. Phys. Oceanogr. **25** (10), 2344–2360 (1995).

12. P. J. Lamb, "On the Mixed Layer Climatology of the North and Tropical Atlantic," Tellus Ser. A **36**, 295–305 (1984).
13. S. J. Lentz, "The Surface Boundary Layer in Coastal Upwelling Regions," J. Phys. Oceanogr. **22** (12), 1517–1539 (1992).
14. S. Levitus, *Climatological Atlas of the World Ocean*, (NOAA Prof. Pap., Vol. 13, U.S. Govt. Print. Off., Washington, DC, 1982).
15. M. R. Lewis, M. Carr, G. Feldman, et al., "Influence of Penetrating Solar Radiation on the Heat Budget of the Equatorial Pacific Ocean," Nature **347** (6293), 543–544 (1990).
16. C. P. Lombardo and M. C. Gregg, "Similarity Scaling of Viscous and Thermal Dissipation in a Convecting Surface Boundary Layer," J. Geophys. Res. **94**, 6273–6284 (1989).
17. I. D. Lozovatsky, A. L. Berestov, and A. S. Ksenofontov, "Phillips Theory of Turbulence-Generated Fine Structure: Numerical and Stochastic Modelin," in *Abstracts of John Hopkins Conference in Environmental Fluid Mechanics, Baltimore MD, 1998*), pp. 102–103.
18. R. Lukas and E. Lindstrom, "The Mixed Layer of the Western Equatorial Pacific," J. Geophys. Res. **96 (**Suppl. S), 3343–3357 (1991).
19. P. J. Martin, "Simulation of Mixed Layer at OWS November and Papa with Several Models," J. Geophys. Res. **90** (C1), 903–916 (1985).
20. J. R. Miller, "The Salinity Effect in a Mixed Layer Ocean Model," J. Phys. Oceanogr. **6** (1), 29–35 (1976).
21. G. Monterey and S. Levitus, *Seasonal Variability of Mixed Layer Depth for the World Ocean* (NOAA Atlas NES-DIS, Vol. 14, U.S. Govt. Print. Off., Washington, DC, 1997).
22. P. P. Niiler and E. B. Kraus, *Modeling and Prediction of the Upper Layers of the Ocean*, Ed. by E. B. Kraus (Pergamon, New York, 1977), pp. 143–172.
23. A. Obata, J. Ishazaka, and M. Endoh, "Global Verification of Critical Depth Theory for Phytoplankton Bloom with Climatological in situ Temperature and Satellite Ocean Color Data," J. Geophys. Res. **101**, 20 657–20 667 (1996).
24. L. Padman and T. M. Dillon, "Turbulent Mixing Near the Yermak Plateau during the Coordinate Eastern Arctic Experiment," J. Geophys. Res. **96**, 4769–4782 (1991).
25. H. Peters, M. C. Gregg, and J. M. Tool, "Meridional Variability of Turbulence Through the Equatorial Undercurrent," J. Geophys. Res. **94**, 18 003–18 009 (1989).
26. R. T. Pollard, P. B. Rhines, and O. R. Y. Thompson, "The Deepening of the Wind-Mixed Layer," Geophys. Fluid Dynamics **3** (4), 381–404 (1973).
27. J. E. Price, R. A. Weller, and R. Pinkel, "Diurnal Cycling: Observations and Models on the Upper Ocean Response to Diurnal Heating, Cooling, and Wind Mixing," J. Geophys. Res. **91**, 8411–8427 (1986).
28. P. Qu, "Mixed Layer Heat Balance in the Western North Pacific," J. Geophys. Res. **108** (3242), 35-1–35-13 (2003) [doi:10.1029/2002JC0015326].
29. K. J. Richards, M. E. Inall, and N. C. Wells, "The Diurnal Mixed Layer and Upper-Ocean Heat Budget in the Western Equatorial Pacific," J. Geophys. Res. **100** (C4), 6865–6879 (1995).
30. N. Schneider and P. Muller, "The Meridional and Seasonal Structures of the Mixed-Layer Depth and Its Diurnal Amplitude Observed During the Hawaii-to-Tahiti Shuttle Experiment," J. Phys. Oceanogr. **20** (9), 1395–1404 (1990).
31. M. A. Spall, "A Diagnostic Study of the Wind- and Buoyancy-Driven North Atlantic Circulation," J. Geophys. Res. **96** (C10), 18 509–18 518 (1991).
32. R. Thompson, "Climatological Numerical Models of the Surface Mixed Layer of the Ocean," J. Phys. Oceanogr. **6** (4), 496–503 (1976).
33. R. G. Wagner, "Decadal Scale Trends in Mechanisms Controlling Meridional Sea Surface Temperature Gradients in the Tropical Atlantic," J. Geophys. Res. **101** (C7) 16 683–16694 (1996).
34. G. L. Weatherly and P. L. Martin, "On the Structure and Dynamics of Oceanic Bottom Boundary-Layer," J. Phys. Oceanogr. **8** (4), 557–570 (1978).
35. S. S. Zilitinkevich and I. N. Esau, "On Integral Measures of the Neutral Barotropic Planetary Boundary Layer," Boundary Layer Meteorol. **104** (3), 371–379 (2002).